ISSN 2176-5480

22nd International Congress of Mechanical Engineering (COBEM 2013)
November 3-7, 2013, Ribeirão Preto, SP, Brazil

NUMERICAL SIMULATION OF SHEET METAL FORMING PROCESS BY LEMAITRE´S DAMAGE MODEL

Raniere Silva Neves
Lucival Malcher
UnB – University of Brasília, Faculty UnB Gama, Distrito Federal – Brazil
raniere_neves@aluno.unb.br
malcher@unb.br

Abstract. *In this paper, it is proposed the control of sheet metal forming process through the analysis of an isotropic damage variable, which is based on Continuum Damage Mechanics, initially suggested by Lemaitre. Regarding the metal forming process, the level of material degradation is established for each thickness of the sheet metal. In the first part of this study, a brief review about the forming processes and the mathematical equation of Lemaitre's model are made. In the second part, Lemaitre's model is implemented in an academic finite element environment for initial tests and then in a commercial software (Abaqus) intending to perform definitive simulations. At the end, the level of internal degradation is evaluated through the relation between the damage level found and the sheet thickness used in the process.*

Keywords: *metal forming process, isotropic damage model, finite elements*

1. INTRODUTION

The Brazilian automotive market has grown considerably in recent decades, to keep up with this increased demand, the automotive industry seeks to invest in manufacturing processes faster and cheaper, can produce large batches of parts with a high level of quality. Because of their advantageous features in series in the manufacture of strong, lightweight metal parts such as: A high dimensional accuracy and low cost, stamping processes have gained popularity in the industrial setting, not only in automotive, but many others.

At its origin, operations stampings attempts were based on practices and empiricism, the tools were made without the use of technical knowledge, which contributed to the production of parts with a low dimensional accuracy. Over time the scope for operations stampings were improved and increased with the construction of stamping tools better, thanks to advances in research on materials.

However, today the control of stamping processes is a complicated task. The complex behavior of tension in the work piece during the forming process makes it difficult to perform appropriate analytical operation, making the appropriate dimensioning of the parameters involved in the process, as required to perform the loading operation, sheet thickness, angle of stamping tools, among others, and making the occurrence of failures during the process commonplace.

The faulty operation may have origins from lack of quality plate material which will be submitted to the process or may result from inadequate sizing of some parameter of the forming process, then the analysis of the origin of defects requires one to have a detailed knowledge of both the process and the material.

Perform quality control of the material of the plate before printing is relatively easy and very widespread nowadays, since the definition of process parameters is not a trivial function.

It is common today, manufacturers are based on trial and error for the operation scale, this approach resembles a process of calibration of the parameters involved in the printing process and can generate a lot of scrap, which means extra costs and increased production time.

An alternative to design and obtain a proper control of stamping operations that has grown in the industrial environment is the use of computational mechanics to simulate the process as a whole. With the aid of a computer can analyze the behavior of materials on specific shipments, recreate scenarios and test the resistance of components without generating scrap and additional costs, and shorten the testing.

There are some possible strategies to define the location and the initiation of a crack at the mesoscopic scale through computational mechanics. However, a simple and easiest solution is to use the so-called critical damage criterion. This criterion states that a crack is initiated when the mesoscopic damage value of the material reaches a critical value (Lemaitre, 2005), according to Equation (1).

$$D > D_C \ , \tag{1}$$

where D is a dimensionless variable that aims to account for the level of degradation of the material, which relates the change in the elastic modulus of the material to the level of degradation, even in the case of constitutive model of Lemaitre and D_C is the value of critical damage . The value of critical damage is regarded as a material constant. Although its value is difficult to determine, for many materials the critical damage value is in the range of 0.2 to 0.5.

ISSN 2176-5480

2. THEORICAL ASPECTS

2.1 Stamping Process

Imprinting is a process of mechanical forming, usually held cold, which is prescribed geometric own a sheet metal by performing a set of operations that may involve cutting and plastic deformation of the material, (Junior and Caversan, 2012).

In general terms the process works in the following way: A plate, or just a strip thereof, is supported on a matrix and by means of a tool, called stamping, installed in a press, a certain force is applied on the material with the intension to cut it by pure shear or assign the shape of the matrix material through plastic deformation.

The stamping plate is used for the manufacture of thin-walled parts, the part can be either hollow or flat, depending on the operations used.

A feature of the product manufacturer is by stamping regions of high mechanical resistance to plastic deformation relative to the initial sheet, becoming very common in the design of large pieces using profiles, shaped plates, ribs or recesses in the part itself to increase its stiffness.

The main advantages of this manufacturing process in relation to others are: High productivity because it is a relatively simple and fast; Cost of production reduced by piece; Parts with good workmanship, parts with greater strength due to conformation, which causes strain hardening of the material, and low cost due to quality control and uniformity of the production facility for detecting deviation during production.

Due to these characteristics, stamping processes have become popular in industry. However, the stamping process also has some disadvantages such as having a high tooling cost, but that cost could be amortized high production pieces. Another limiting factor for the process is the type of material to be printed. Due to the characteristics of the stresses involved in the operations of stamping, the stamping process is restricted to homogeneous metallic materials with sufficiently fine grain and good toughness, that is, materials capable of withstanding relatively well to rupture and not very high stiffness so that wrinkles are not generated during operations. To perform any stamping operation, it is also essential that the raw material is in the form of sheets or ribbons.

The most commonly used materials in stamping plates are low carbon steels that for deep drawing operations, should provide a good resistance to breakage. Other materials commonly used in this process are copper, aluminum, stainless steel and zinc and 70-30 brass (alloy of copper with 30% zinc), material that has one of the highest rates of formability, and is therefore used in parts whose requirements justify the selection of material high cost.

The stamping operations can be described by two main types of operations: the separation of the material and the change in shape of the material. The separation operations cover material cutting and modification operations include the operations of the form of plastic deformation.

In the cutting operation is desired that internal tensions in specific regions of the plate exceed the breaking point of the material, causing the appearance of cracks and fissures, which subsequently result in separation of the material. Already in the forming operation is only desirable that the material permanently deform if any internal stresses in the region of the part exceeding the breaking point of the material, cracks arise and the workpiece becomes useless, it is necessary to carry out appropriate control of deformation

2.2 Lemaitre´s model with isotropic damage

The Lemaitre constitutive model based on the concept of effective stress and strain equivalence hypothesis and includes the non-linear isotropic hardening and kinematic description of the behavior of ductile metals undergoing efforts.

Other remarkable features of this constitutive model are: the fact that it is insensitive to pressure and it does not make difference between compressive stresses of tensile stresses acting on a component.

The formulation of the model is based on the hypothesis of a potential state or thermodynamic potential, which are derived from state laws. In this case, the Helmholtz free energy can be understood as a potential state of the material and adopted to solve the problem. The free energy can be expressed as a function of the set $\{\boldsymbol{\varepsilon^e}, r, \boldsymbol{\beta}, D\}$ of state variables according to equation (2):

$$\psi = \psi(\boldsymbol{\varepsilon^e}, r, \boldsymbol{\beta}, D)\,, \tag{2}$$

where ψ is the specific free energy, $\boldsymbol{\varepsilon^e}$ is the elastic strain tensor, r is the internal variable hardening isotropic, D is the damage variable β is isotropic and the internal variable related to kinematic hardening.

In this case, the process is assumed to be isothermal, and then the choice of internal variables depends on the physical phenomenon under study (elasticity, isotropic and kinematic hardening, and damage).

ISSN 2176-5480

Adopting the hypothesis that the damage affects only the elastic component, it is possible to place a decoupling of the ideas of elastic damage and plastic hardening, so the specific free energy happens to be rewritten in the form of Equation (3) as:

$$\psi = \psi^{ed}(\boldsymbol{\varepsilon^e}, D) + \psi^{p}(r, \boldsymbol{\beta}) \,, \tag{3}$$

where ψ^{ed} represents the contribution of the elastic damage and ψ^{p} is the plastic contribution to the free energy. In this theory, the elastic potential damage can be defined by Equation (4) as:

$$\bar{\rho}\psi^{ed}(\boldsymbol{\varepsilon^e}, D) = \frac{1}{2}\boldsymbol{\varepsilon^e}\colon(1-D)\boldsymbol{D^e}\colon\boldsymbol{\varepsilon^e} \;, \tag{4}$$

where $\boldsymbol{D^e}$ represents the isotropic elasticity matrix. In this case, the linear elastic law is obtained by derived from potential damage due to elastic strain tensor, according to Equation (5).

$$\boldsymbol{\sigma} = \bar{\rho}\frac{\partial\psi^{ed}}{\partial\boldsymbol{\varepsilon^e}} = (1-D)\boldsymbol{D^e}\colon\boldsymbol{\varepsilon^e} \;. \tag{5}$$

The thermodynamic forces, Y, associated with the internal variables of damage and isotropic hardening is obtained by derived from elastic damage potential due the damage variable, according to Equation (6).

$$Y \equiv \bar{\rho}\frac{\partial\psi^{ed}}{\partial D} = -\frac{1}{2}\boldsymbol{\varepsilon^e}\colon\boldsymbol{D^e}\colon\boldsymbol{\varepsilon^e} \;. \tag{6}$$

After some mathematical manipulations, the thermodynamic forces can be defined as a function of hydrostatic pressure, p, and von Mises equivalent stress, q, as in Equation (7).

$$Y = \frac{-q^2}{6G(1-D)^2} - \frac{p^2}{2K(1-D)^2} \;, \tag{7}$$

where G is the shear modulus, K is the bulk modulus and q is von Mises equivalent stress, which is defined by Equation (8) as

$$q = \sqrt{\frac{3}{2}\boldsymbol{S}\colon\boldsymbol{S}} = \sqrt{3J_2} \;, \tag{8}$$

where $\boldsymbol{S}$ is the deviatoric stress tensor and J_2 represents the second invariant of the deviatoric stress tensor. Nevertheless, the plastic contribution to the free energy can be expressed by Equation (9) as the sum of different contributions related to the isotropic and kinematic hardening:

$$\bar{\rho}\psi^{p}(r, \boldsymbol{\beta}) = \bar{\rho}\psi^{I}(r) + \frac{a}{2}\boldsymbol{\beta}\colon\boldsymbol{\beta} \;, \tag{9}$$

where $\bar{\rho}\psi^{I}(r)$ is an arbitrary function of r and a is a material constant related to kinematic hardening. The thermodynamic force associated with isotropic hardening material is defined by Equation (10) and associated with the kinematic hardening by Equation (11).

$$R \equiv \bar{\rho}\frac{\partial\psi^{p}(r,\boldsymbol{\beta})}{\partial r} = \bar{\rho}\frac{\partial\psi^{I}(r)}{\partial r} = R(r) \,, \tag{10}$$

$$\boldsymbol{X} \equiv \bar{\rho}\frac{\partial\psi^{p}(r, \boldsymbol{\beta})}{\partial\boldsymbol{\beta}} = a\boldsymbol{\beta} \,, \tag{11}$$

where $\boldsymbol{X}$ represents the so-called back-stress tensor. After defining the entire state and the corresponding variables associated to the model of Lemaitre, the evolution of the internal variables can be obtained by assuming the existence of a single dissipation potential, Ψ, given by Equation (12):

$$\Psi = \Psi(\boldsymbol{\sigma}, R, \boldsymbol{X}, Y, \boldsymbol{\varepsilon^e}, \boldsymbol{r}, \boldsymbol{\beta}, D) \,. \tag{12}$$

ISSN 2176-5480

According to the approach of a unique dissipation potential and applying the Legendre-Fenschel transformation, the so-called complementary dissipation potential is given by the additive decomposition of hardening, Ψ^p, and damage, Ψ^d, in the form of Equation (13).

$$= {}^{p} + {}^{d} = + \frac{b}{2a}\boldsymbol{X}:\boldsymbol{X} + \frac{S}{(1-D)(s+1)}.\left(\frac{-Y}{S}\right)^{s+1} , \tag{13}$$

where a, b, S and s are material constants and Φ represents the yield criterion of Lemaitre´s model defined by Equation (14) as:

$$\Phi(\boldsymbol{\sigma}, \boldsymbol{X}, R, D) = \frac{\sqrt{3J_2(\boldsymbol{S}-\boldsymbol{X})}}{(1-D)} - \sigma_{yo} - R(r), \tag{15}$$

where σ_{yo} is the yield stress of the material analyzed. According to the hypothesis of generalized normality, the plastic flow rule for the model is given by Equation (16) as:

$$\dot{\boldsymbol{\varepsilon}}^p = \dot{\gamma}\frac{\partial \Psi}{\partial \boldsymbol{\sigma}} = \dot{\gamma}\boldsymbol{N} , \tag{16}$$

where $\dot{\gamma}$ represents the plastic multiplier and $\boldsymbol{N}$ is the so-called flow vector, defined by Equations (17), as follow:

$$\boldsymbol{N} = \sqrt{\frac{3}{2}}\frac{(\boldsymbol{S}-\boldsymbol{X})}{(1-D)\|\boldsymbol{S}-\boldsymbol{X}\|} . \tag{17}$$

The evolution laws of the internal variables for the damage, isotropic and kinematic hardening are established by the equations (18), (19) and (20), respectively.

$$\dot{D} \equiv \dot{\gamma}\frac{\partial \Psi}{\partial Y} = \dot{\gamma}\frac{1}{(1-D)}.\left(\frac{-Y}{S}\right)^{s} , \tag{18}$$

$$\dot{r} \equiv -\dot{\gamma}\frac{\partial \Psi}{\partial R} = \dot{\gamma} , \tag{19}$$

$$\dot{\boldsymbol{\beta}} = \dot{\gamma}\frac{\partial \Psi}{\partial \boldsymbol{X}} = \dot{\gamma}(a\boldsymbol{N} - b\boldsymbol{X}) . \tag{20}$$

In order to ensure that the model works correctly, supplementary laws represented by Equation (21) must also be met:

$$\dot{\gamma} \geq 0 , \qquad \Phi \leq 0 , \qquad \dot{\gamma}\Phi = 0 . \tag{21}$$

The equivalent plastic strain rate is calculated from the previous equation as expressed in Equation (22).

$$\dot{\bar{\boldsymbol{\varepsilon}}}^p = \frac{\dot{\gamma}}{(1-D)} . \tag{22}$$

Thus the law of damage evolution can be rewritten as Equation (23).

$$\dot{D} = \dot{\bar{\boldsymbol{\varepsilon}}}^p \left(\frac{-Y}{S}\right)^{s} . \tag{23}$$

The mathematical equation of the constitutive model of Lemaitre is presented in summary form in Table 1.

ISSN 2176-5480

Table 1 – Lemaitre´s model with isotropic and kinematic hardening, and damage.

i. Additive decomposition of strain tensor:

$$\boldsymbol{\varepsilon} = \boldsymbol{\varepsilon}^e + \boldsymbol{\varepsilon}^p$$

ii. Elastic law with damage coupled:

$$\sigma = (1 - D)\boldsymbol{D}^e : \boldsymbol{\varepsilon}^e$$

iii. Yield criterion:

$$\Phi = \frac{q}{(1 - D)} - \sigma_{yo} - R(r)$$

iv. Plastic flow rule $\dot{\boldsymbol{\varepsilon}}^p$ and evolution equations for the internal variables r, $\boldsymbol{\beta}$ e D

$$\dot{\boldsymbol{\varepsilon}}^p = \dot{\boldsymbol{\gamma}}\boldsymbol{N} = \dot{\boldsymbol{\gamma}}\sqrt{\frac{3}{2}}\frac{(\boldsymbol{S} - \boldsymbol{X})}{(1 - D)\|\boldsymbol{S} - \boldsymbol{X}\|}$$

$$\dot{r} = \dot{\gamma}$$

$$\dot{\boldsymbol{\beta}} = \dot{\gamma}(a\boldsymbol{N} - b\boldsymbol{X})$$

$$\dot{D} = \dot{\gamma}\frac{1}{(1 - D)} \cdot \left(\frac{-Y}{S}\right)^S$$

with Y:

$$-Y = \frac{q^2}{6G(1-D)^2} + \frac{p^2}{2K(1-D)^2}$$

v. Complementary equations

$$\dot{\gamma} \geq 0 \qquad \Phi \leq 0 \qquad \dot{\gamma}\Phi = 0$$

3. NUMERICAL STRATEGY

3.1 Return mapping algorithm

For the simulations is necessary to transform the mathematical model of Lemaitre presented in the previous section in a computational model as an integration algorithm that will be implemented in a finite element tool.

The numerical integration of Lemaitre model is based on return mapping strategy that was originally proposed by Benallal et al. (1988), and Doghri and Billardon (1995) considering the hypothesis of small strain and later expanded by several researchers, considering large strain (De Souza Neto, 1994:1998; Saanouni, 2000). The numerical integration algorithm proposed originally (see Benallal et al., 1988) carried, in a three-dimensional problem, a system of fifteen non-linear scalar equations, solved iteratively according to the Newton-Rapshon method. Analyzing the return mapping procedure (Simo, 1998), the original integration algorithm has been reduced for a non-linear system of two equations, in an isotropic hardening case (Saanouni, 2007). A major simplification for the same was suggested by De Souza Neto (2002), given the resolution of only one scalar non-linear equation for the plastic multiplier, γ.

The use of path-dependent constitutive models, such as the original Lemaitre´s model, invariably leads to the need for devising algorithms for numerical integration of the evolution equations. The problem then is to formulate the following numerical integration to be able to update the internal variables of the process, generally denoted by α_n, at time t_n, for determine the internal variables α_{n+1}, at time t_{n+1}, where the increased strain, $\Delta\varepsilon$, is assumed known.

Further, the discretization of the constitutive model, in the so-called pseudo-time $[t_n, t_{n+1}]$ is applied based on the Euler backward scheme (Simo and Hughes, 1998). Since the model is implemented in a quasi-static finite element program, it is also necessary to derive the consistent tangent matrix with the integration algorithm. The procedure of updating the stress tensor, which is based on the so-called operator split methodology (Simo and Hughes, 1998; De Souza Neto et al. 2008) has been used extensively in computational plasticity and consists in dividing the problem into two parts: an elastic predictor, which mounts a trial state assuming the problem as completely elastic, and a plastic corrector, where from the violation of the yield stress criterion, makes a correction in the trial state previously constructed. Then, in this step, a system of non-linear equations formed by the update equation for the stress tensor, the

ISSN 2176-5480

yield criterion and the evolution equations for the internal variables is solved. The return mapping algorithm for Lemaitre´s model is summarized in Table 2.

Table 2 – Return mapping for Lemaitre´s model with isotropic hardening and isotropic damage.

i. Determine the trial state (elastic predictor): Given an incremental strain, $\Delta\varepsilon$, and the internal variables at pseudo-tempo t_n:

$$\boldsymbol{\varepsilon}_{n+1}^{e\,trial} = \boldsymbol{\varepsilon}_n + \Delta\boldsymbol{\varepsilon}\,;\; R_{n+1}^{trial} = R_n;\; D_{n+1}^{trial} = D_n$$

$$\tilde{\boldsymbol{S}}_{n+1}^{trial} = 2G\boldsymbol{\varepsilon}_{n+1}^{e\,trial};\; \tilde{p}_{n+1} = K\varepsilon_{v\,n+1}^{e\,trial};\; \tilde{q}_{n+1}^{trial} = \sqrt{\frac{3}{2}}\left\|\tilde{\boldsymbol{S}}_{n+1}^{trial}\right\|/(1-D_n)$$

ii. Plastic admissibility:

if $\Phi^{trial} = \tilde{q}_{n+1}^{trial} - \sigma_{y0}^{trial}(R_{n+1}^{trial}) \leq 0$ then

$(*)_{n+1} = (*)_{n+1}^{trial}$ (elastic regime) and END (*v*)

Elseif (Plastic regime) go to return mapping

iii. Return mapping algorithm (Plastic corrector): Solve the system of non-linear equations for $\Delta\gamma$, using the Newton-Raphson method.

$$F(\Delta\gamma) \equiv \omega(\Delta\gamma) - \omega_n + \frac{\Delta\gamma}{\omega(\Delta\gamma)}\left(\frac{-Y(\Delta\gamma)}{S}\right)^s = 0$$

where,

$$\omega(\Delta\gamma) = 1 - D_{n+1} = \frac{3G\Delta\gamma}{\tilde{q}_{n+1}^{trial} - \sigma_y(R_n + \Delta\gamma)}$$

$$-Y(\Delta\gamma) \equiv \frac{\left[\sigma_{y0}(R_n + \Delta\gamma)\right]^2}{6\mathrm{G}} + \frac{\tilde{p}_{n+1}{}^2}{2K}$$

iv. Updating the other state variables:

$$R_{n+1} = R_n + \Delta\gamma;\; p_{n+1} = \omega(\Delta\gamma) + \tilde{p}_{n+1};\; \boldsymbol{S}_{n+1} = \frac{q_{n+1}}{\tilde{q}_{n+1}^{trial}}\tilde{\boldsymbol{S}}_{n+1}^{trial}$$

$$\boldsymbol{\varepsilon}_{n+1}^{e} = \frac{1}{2G}\boldsymbol{S}_{n+1} + \frac{1}{3}\boldsymbol{\varepsilon}_{v\,n+1}^{e\,trial}\boldsymbol{I};\; q_{n+1} = \omega(\Delta\gamma) + \sigma_{y0}(R_{n+1});\; \boldsymbol{\sigma}_{n+1} = \boldsymbol{S}_{n+1} + p_{n+1}\boldsymbol{I}$$

v. **END**

3.2 Numerical example

The integration algorithm proposed in the previous section was implemented in ABAQUS Standard (UMAT rotine). In order to conduct this work, it was selected, in the literature, an example of deep drawing operation regarding the making of a glass cylindrical elements using two-dimensional axisymmetric. The stamping operation was simulated with seven different sheet thicknesses. The thicknesses of the plates varied from 0.25 mm for the first simulation, up to 1.5 mm in the seventh and last simulation. Were used immediately sheet thicknesses of 0.25 mm, 0.5 mm, 0.75 mm, 0.82 mm, 1.0 mm, 1.25 mm and 1.5 mm, in sequence for the seven simulations.

The simulations were performed with the intention of analyzing the evolution of the damage variable coupled with Lemaitre constitutive model for each configuration sheet, so that the end of the simulations, set the plate thickness appropriate for the operation based on the values obtained for the variable damage.

In the simulations, it was used a blank with initial circular radius of 100 mm, the punch used was designed with a radius of 50 mm and its corners were rounded with a radius of 13 mm, the inner radius of the die also varied to the simulations with sheet thickness larger. Initially, the die has an inner radius of 56.25 mm to the simulations with sheet thicknesses of 0.25 mm, 0.5 mm, 0.75 mm, 0.82 mm and 1.0 mm, to the simulations with sheet thicknesses of 1.25 the die has an inner radius of 56.5 mm and 56.75 mm to the simulation with sheet thicknesses of 1.5 mm. However, the

ISSN 2176-5480

settings for all the corners of the array have been rounded with a radius of 5 mm. The geometry of the problem is shown in Figure 1.

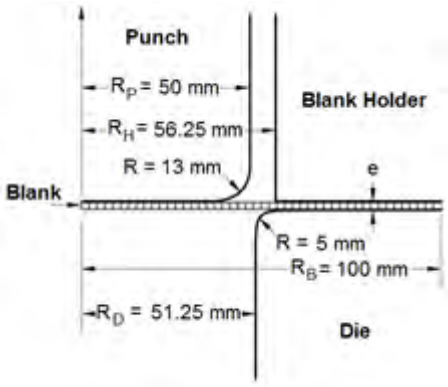

Figure 1. Geometry for a deep drawing operation.

At the start of the analysis for the blank is positioned precisely on top of the die and the blank holder is precisely in touch with the top surface of the blank. The punch is positioned 0.18 mm above the top surface of the blank.

The blank is modeled using 40 elements of type CAX4R, a 4-node reduced-integration axisymmetric quadrilateral element, allowing the symmetry of the set was used for only half the problem was recreated in 2D. While the rigid punch, the die, and the blank holder were modeled as analytical rigid surfaces with the *RIGID BODY option in conjunction with the *SURFACE option.

Another point of the simulations are the meshes used. These meshes are rather coarse for this analysis. However, since the primary interest in this problem is to study the membrane effects, the analysis will still give a fair indication of the stresses and strains occurring in the process.

The mechanical interaction between the contact surfaces is assumed to be frictional contact. Therefore, the *FRICTION option is used in conjunction with the various *SURFACE INTERACTION property options to specify coefficients of friction and was used the surface-to-surface contact formulations to realization of calculations.

The coefficient of friction between the interface and the punch is taken to be 0.25 and that between the die and the blank holder is taken as 0.1, simulating a certain degree of lubrication between the surfaces. The stiffness method of sticking friction is used in these analyses.

To the confection of the sheets was used aluminum-killed steel with material, satisfying the Ramberg-Osgood relation between true stress and logarithmic strain, expressed in the Equation (24):

$$\varepsilon = \left(\frac{\sigma}{K}\right)^{1/n} \tag{24}$$

All the parameters mentioned in the Equation (24) are conveniently listed in Table 3.

Table 3 - Material properties for the aluminum-killed steel

Description	Symbol	Value
Elastic Modulus	E	211 GPa
Poisson's ratio	υ	0.3
Initial yield stress	σ_{y_0}	91.3 MPa
Reference stress value	K	513 MPa
Work-hardening exponent	n	0.223

All simulations were carried out in three steps. The analysis of the effect springback effect has been disregarded in the simulation since this springback in the CAX4R model is not physically realistic, since the reduced integration elements have a purely flexural elastic behavior.

- In the first step the blank holder is pushed onto the blank with a prescribed displacement to establish contact;
- In the second step the boundary condition is removed and replaced by the applied force of 100 kN on the blank holder. This force is kept constant during Steps 2 and 3. This technique of simulating the clamping process is used to avoid potential problems with rigid body modes of the blank holder, since there is no firm contact

ISSN 2176-5480

between the blank holder, the blank, and the die at the start of the process. The two-step procedure creates contact before the blank holder is allowed to move freely;

- In the third step the punch is moved toward the blank through a total distance of 60 mm. This step models the actual drawing process.

4. RESULTS

The Figure 2 shows a plot of Maximum Equivalent Plastic Strain achieved for each simulation in function of the thickness of sheet used during the simulation.

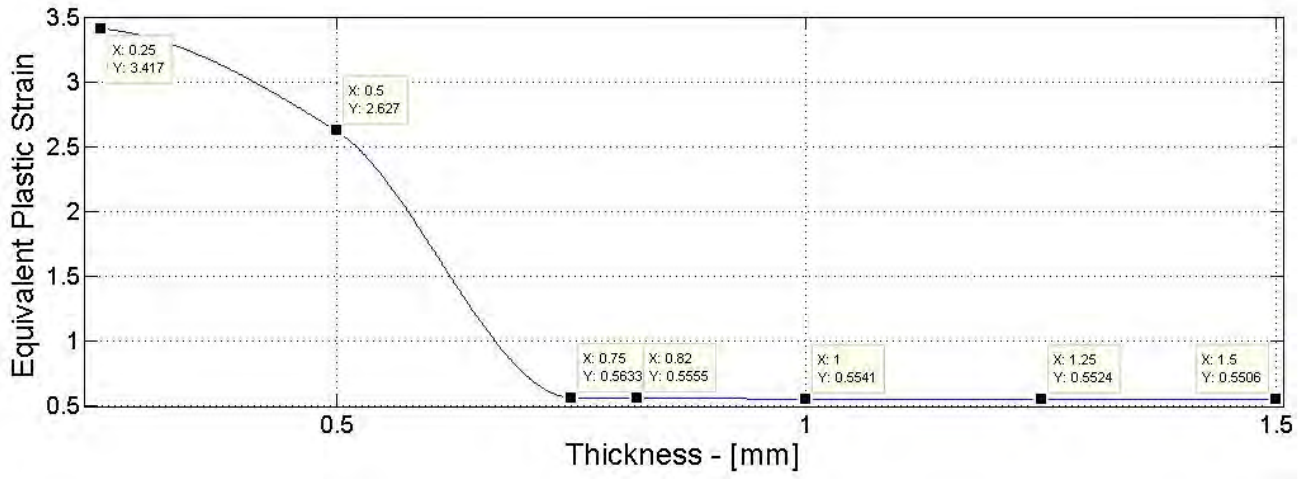

Figure 2. Plot Maximum Equivalent Plastic Strain according of the sheet thickness

To analyze the behavior of the plate during operation, were captured images of the von Mises equivalent stress (a), Third invariant (b) and Equivalent Plastic Strain (c) present on the sheet at the end of the simulation using thickness of the sheet: 0.5 mm, 0.82 mm and 1.5 mm, as show at the Figures (3), (4) and (5), respectively:

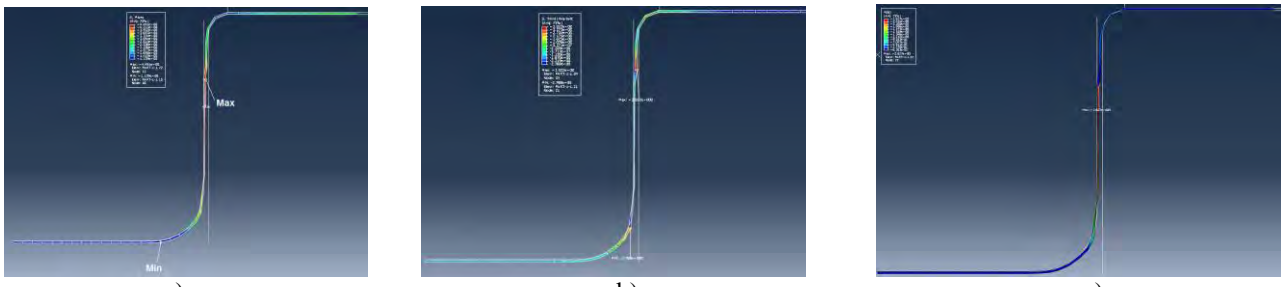

a) b) c)

Figure 3. Results to simulation used a thickness of sheet of 0.5 mm

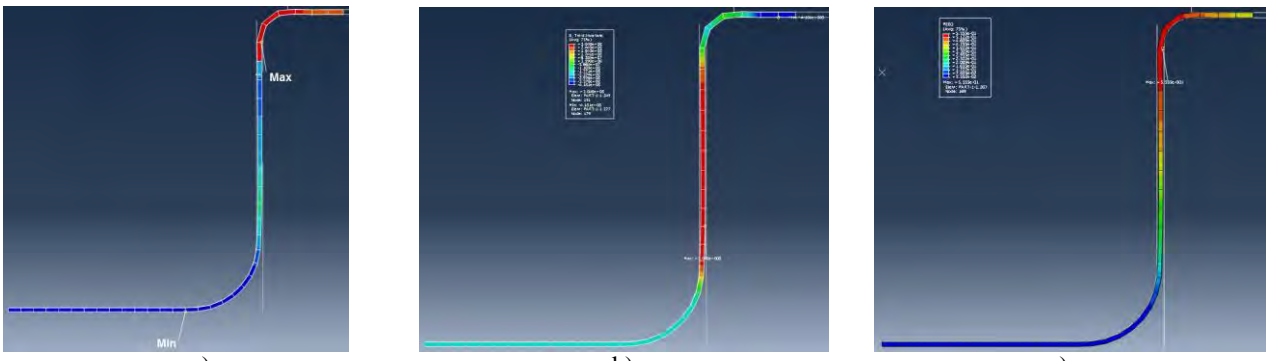

a) b) c)

Figure 4. Results to simulation used a thickness of sheet of 0.82 mm

ISSN 2176-5480

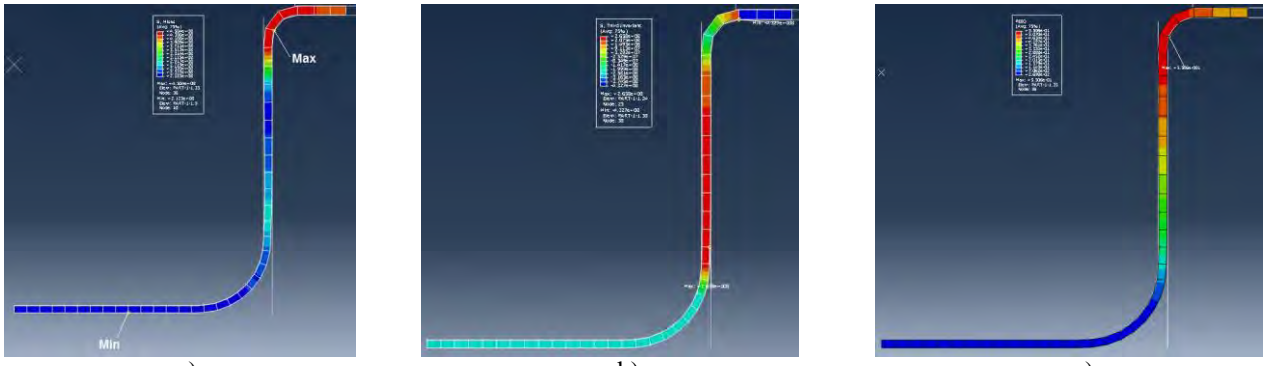

a) b) c)

Figure 5. Results to simulation used a thickness of sheet of 1.5 mm

These sheet thickness were chosen because they represent keypoints in Figure 2. The simulation with sheet thickness of 0.5 mm represents the simulation where the sheet does not support the advancement of the punch, the simulation with sheet thickness of 0.82 mm represents the firt simulation where the Maximum Equivalent Plastic Strain achieves the standard, about 0.555, and lastly, the simulation with sheet thickness of 1.5 mm represents the last simulation carried out.

5. CONCLUSION

The plot of the Figure (2) shows that from the simulation with sheet thickness of 0.82 mm the Equivalent Plastic Strain achieves a standard. This means that to perform a correctly stamping, the sheet thickness should be greater than or equal to 0.82 mm, otherwise the sheet will break.

Therefore, concludes that it is possible using a finite element academic tool and recreating the appropriate boundary conditions to conduct trials of sheet metal forming.

6. REFERENCES

Alves, J.L.C.M. “Simulação Numérica do Processo de Estampagem de Chapas Metálicas: Modelagem Mecânica e Métodos Numéricos”. 2003. 368 p. Tese (Doutorado em Engenharia Mecânica) – Departamento de Engenharia Mecânica, Universidade do Minho, Guimarães. 2003.

Button, S.T., Bortolussi, R. “Estudo do Processo de Embutimento Profundo de Copo Pelo Método dos Elementos Finitos”. *Engenharia Mecânica*: UNICAMP, Campinas, v. 21, n. 2, p. 355-363, 1999.

De Souza Neto, E.A., Peri´c, Owen, D.R.J. “Computational methods for plasticity: theory and applications”. John Wiley & Sons Ltd, 2008.

Filho, E.B., Silva, I.B., Batalha, G.F., Button, S.T. “Conformação plástica dos metais”. 6. ed. São Paulo: EPUSP, 2011. 254 p.

Franco, E., Lino, J.C., Kamel, K. et al. “Estampagem dos Aços”. São Paulo: Associação Brasileira de Metais.

Junior, I.B., Caversan, E.G. “Tecnologia de Estampagem 1: Corte”. São Paulo: Faculdade de Tecnologia de Sorocaba, 2012. 82 p.

Lemaitre, J. “A continuous damage mechanics model for ductile fracture”. In *Journal of Engineering Materials and Technology - Trans. of the ASME*, 107, 1985. p. 83–89.

Malcher, L., Andrade Pires, F.M., César de Sá, J.M.A. “An Assessment of Isotropic Damage Constitutive Models under High and Low Stress Triaxialities”. In *International Journal of Plasticity*, 2011.

Malcher, L. “Da Mecânica do Dano Contínuo: Uma evolução do modelo de Lemaitre para redução da dependência do ponto de calibração”. 2011. 122 p. Tese (Doutorado em Ciências Mecânicas) – *Departamento de Engenharia Mecânica*, Universidade de Brasília, Brasília. 2011.

Mesquita, E.L.A., Rugani, L.L. “Estampagem dos aços inoxidáveis”, Acesita S.A., 1997.

Palmeira, A.A. “Capítulo 8: Processos de Estampagem”. 2005. 50 p. Dissertação (Mestrado em Engenharia de Produção ênfase em produção mecânica) – *Departamento de mecânica e energia*, Universidade do Estado do Rio de Janeiro, Resende. 2005.

Penteado, F. “Processos de Estampagem”, 2010.

Predabon, E.P. “Conformando Melhor o Tempo Time Being Better Conforming”. In *CONFERÊNCIA NACIONAL DE CONFORMAÇÃO DE CHAPAS, 7., 2004*, Porto Alegre. *Anais...* Porto Alegre, 2004. p. 169 – 180.

Provenza, F. “Conformação Mecânica”. São Paulo: Escola Protec, 1985.

Rosa, R.H.L., Ávila, A.F., Campos, H.B., Pertence, A.E.M., Cetlin, P.R "Influencia da Restrição no Fluxo Metálico na Localização da Região de Falha na Estampagem de Chapas". In *SENAFOR, 23., 2004*, Porto Alegre. *Anais...* Porto Alegre, 2004. p. 103 - 114.

Saanouni, K., K. Nesnas and Y. Hammi. "Damage modeling in metal forming processes". In *International Journal of Damage Mechanics 9(3), 2000*. p. 196-240.

Schaeffer, L. "Fundamentos do projeto de ferramentas para o processo de estampagem". Porto Alegre: Universidade Federal do Rio Grande do Sul, p. 39-44, 2006.

SENAI. "Tecnologia Mecânica". São Paulo: Supervisor de 1ª linha, 1999.

Teixeira, P.M.C. "Ductile Damage Prediction in Sheet Metal Forming and Experimental Validation". 2010. 231 p. Tese (Pós-doutorado em Engenharia Mecânica) – *Faculdade de Engenharia da Universidade do Porto*, Porto. 2010.